Androgen Receptor Phosphorylation at Serine 81 and Serine 213 in Castrate-Resistant Prostate Cancer

Running Title: AR phosphorylation and prostate cancer

Milly J. McAllister (m.mcallister.1@research.gla.ac.uk)[1], Pamela McCall (pamela.mccall@sbdrugdiscovery.com)[1], Ashley Dickson (ashley.dickson@hotmail.com)[1], Mark A. Underwood (Mark.Underwood@ggc.scot.nhs.uk)[2], Ditte Andersen (ditteandersen@bioclavis.co.uk)[3], Elizabeth Holmes (elizabethsutton@bioclavis.co.uk)[3], Elke Markert (elke.markert@glasgow.ac.uk)[4], Hing Y. Leung (h.leung@beatson.gla.ac.uk)[1, 2, 4] and Joanne Edwards (Joanne.Edwards@glasgow.ac.uk)[1]

[1] Unit of Gastrointestinal Cancer and Molecular Pathology, Institute of Cancer Sciences, College of Medical, Veterinary, and Life Sciences, University of Glasgow, Glasgow, G61 1QH

[2] Department of Urology, Queen Elizabeth University Hospital, Glasgow, G31 2ER

[3] BioClavis Ltd, Glasgow, G51 4TF

[4] Cancer Research UK Beatson Institute, Glasgow, G61 1BD

Key Words: Prostate cancer, androgen receptor, phosphorylation, immunofluorescence

Additional information:

Funded by Prostate Cancer UK (S14-003)

Corresponding Author: Milly McAllister t: 07495844591 e: m.mcallister.1@research.gla.ac.uk

Abstract

Background: Despite increases in diagnostics and effective treatments, over 300 000 men die from prostate cancer highlighting the need for specific and differentiating biomarkers. AR phosphorylation associates with castrate-resistance, with pAR^{ser213} promoting transcriptional activity. We hypothesise that combined pAR^{ser81} and pAR^{ser213} reduces survival and would benefit from dual-targeting androgen-dependent and Akt-driven disease.

Methods: Immunohistochemistry and immunofluorescence was performed on matched hormone-naïve and castrate-resistant prostate cancer samples. TempO-Seq gene profiling was analysed using DESeq2 package. LNCaP-AI cells were stimulated with DHT or EGF. WST-1 assays were performed to determine effects of Enzalutamide and BKM120 on cell viability.

Results: Following the development of castrate-resistance, pAR^{ser81} expression reduced and pAR^{ser213} expression increased. Castrate-resistance pAR^{ser81} expression was not associated with survival but high pAR^{ser213} expression was associated with reduced survival from relapse. Combined high pAR^{ser81} and pAR^{ser213} was associated with reduced survival from relapse. pAR^{ser81} expression was induced by 10nM DHT or 10nM EGF and pAR^{ser213} expression was induced by treatment with 10nM EGF in LNCaP-AI cells. Cell viability was reduced following treatment with 10nM Enzalutamide and 10nM BKM120. 8 genes were differentially expressed between hormone-naïve and castrate-resistant tumours and 25 genes were differentially expressed between castrate-resistant tumours with high and low pAR^{ser213} expression.

Conclusion: Combined pAR^{ser81} and pAR^{ser213} provides a novel prognostic biomarker for castrate-resistant disease and a potential predictive and therapeutic target for prostate cancer. Further studies will be required to investigate the combined effects of targeting AR and PI3K/AKT signaling.

Introduction

Prostate cancer (CaP) accounts for over 47 000 new UK diagnoses each year (1). The androgen receptor (AR) plays vital roles in CaP; therefore, current therapies aim to inhibit AR activation directly or indirectly by depleting androgens via androgen deprivation therapy (ADT). Despite a 90% success rate, almost all locally advanced and metastatic patients relapse within 24-36 months and develop castrate-resistant prostate cancer (CRPC). Loss of responsiveness to hormonal therapies is the main challenge facing CaP management (2).

AR phosphorylation, including serine 81 and 308 are linked to AR nuclear-cytoplasmic shuttling and CaP progression (3). Serine 81 is the most common AR phosphorylated site (pAR^{ser81}) and associates with AR transcriptional activity. In the presence of androgens, pAR^{ser81} occurs by cyclin-dependent kinases (CDKs), such as CDK1 and 9, which sensitize AR to low levels of adrenal androgens (4). However, in the absence of androgens, pAR^{ser81} may occur by alternative kinases and reactivate AR signalling.

Recently, androgen-independent AR activation has been proposed as a mechanism for castrate-resistance. Phosphatidylinositol 3-OH kinase (PI3K)/Akt signaling associates with phosphorylated AR serine 213 (pAR^{ser213}), resulting in AR stability (5). We have previously demonstrated *in vitro* upregulation of PI3K/Akt signalling at castrate-resistance and increased pAR^{ser213} expression. Furthermore, we demonstrated an increase in pAR^{ser213} expression in the transition from hormone-naïve to CRPC, this increase was also associated with decreased cancer specific survival from relapse (6). However, no mechanistic analysis or analysis of differential gene expression profiles were conducted for the differing roles of AR phosphorylation at the different sites.

Epidermal growth factor receptor (EGFR) associates with PI3K/Akt activation and CRPC. We previously reported that EGFR variant III (EGFRvIII), a constitutively activated form of EGFR, associates with CRPC. EGFRvIII activates PI3K/Akt signalling, with EGFRvIII and loss of PTEN being

prevalent in CaP, suggesting an androgen-independent mechanism for pAR^{ser81} and pAR^{ser213} expression (6, 7). However, despite no causative relationship observed between EGFRvIII and pAR^{ser81}, EGFRvIII expression reduces CDK inhibitors and activates the cell cycle. As pAR^{ser81} expression is mediated by CDKs, it is hypothesized that EGFRvIII activates CDK expression and increases pAR^{ser81}, however this remains to be identified. A Phase II clinical trial combined the anti-androgen, Enzalutamide, with the PI3K-inhibitor, BKM120, to target both pathways simultaneously. However, PSA was only reduced in 23% of patients and adverse effects occurred. Armstrong *et al* concluded more predictive biomarkers would improve study outcome (8).

Therefore, this study aimed to determine the use of pAR^{ser81} and pAR^{ser213} as prognostic biomarkers and whether these sites could be exploited as dual therapeutic targets and utilised as predictive biomarkers for CRPC. Furthermore, by defining genes associated with AR phosphorylation status future pathway analysis could identify novel and precise targets for these patients.

Materials and Methods

Cell Culture

LNCaP-androgen-independent ((LNCaP-AI) grow in the absence of androgens) cells were gifted from Professor Craig Robson (University of Newcastle) and maintained in phenol red RMPI 1640 supplemented with 10% charcoal-treated foetal calf serum. Media was supplemented with penicillin, streptomycin, and L-Glutamine (Life Technologies, UK).

Antibody Specificity

Antibody specificity for pAR^{ser81} and pAR^{ser213} was previously confirmed (6, 9). In brief, Willder *et al* performed peptide competitive assays to confirm the specificity of pAR^{ser81} phosphorylation site using the peptide with the protein sequence QQQQQQET(pS)PRQQ raised in a rabbit (EZbiolab Inc, USA) at 1:1 and incubated with the pAR^{ser81} antibody (#07-1375; Merk Millipore, USA) overnight at 4° before performing immunohistochemistry as below. Additionally, McCall *et al* performed western blots for pAR^{ser213} (#IMG-561; Imgenex, USA) (also termed pAR^{ser210}) to determine antibody specificity. This was followed by confirming that the pAR^{ser213} antibody only detected the phosphorylated protein by destroying phosphorylated proteins with calf intestinal alkaline phosphatase. One treated slide plus one untreated slide was stained with pAR^{ser213} using immunohistochemistry as below.

Time course drug treatment

LNCaP-AI cells were stimulated and/ or inhibited by 10nM DHT, 10nM EGF, 10nM Enzalutamide and/ or 10nM BKM120 over 1 and 12 hours.

Immunofluorescence

Immunofluorescence was performed as described (10). pAR^{ser81} and pAR^{ser213} antibodies were incubated overnight at 4°C at 1:1000 and 1:200 respectively and visualised using the Zeiss LSM 780 Confocal (Zeiss, Germany). Pixel intensity was quantified using ImageJ, with 10 images taken per experiment performed to n=3 and statistical analysis was performed using one-way ANOVA with Bonferroni correction and Dunnett's test.

WST Proliferation Assay

WST-1 proliferation assays (Roche Diagnostics, Germany) were performed on LNCaP-AI cells to n=3 according to manufacturer's instructions. Statistical analysis was performed using one-way ANOVA with Bonferroni correction and Dunnett's test.

Patients

In total, 109 patients with matched hormone-naïve (HN) and castrate-resistant (CR) tumour pairs were included within this study (diagnosed between 1984-2000 with locally advanced or metastatic CaP from Greater Glasgow and Clyde Health Board). Ethical approval was acquired from Multicentre Research Ethics Committee for Scotland (MREC/01/0/36) and Local Research and Ethics Committees. Patients were selected based on their response to hormone treatment (sub-capsular bilateral orchidectomy or LHRH agonists combined with antiandrogens) and their relapse (2 rises in PSA >10%). HN tissue was obtained via trans-rectal ultrasound guided biopsies and CR tissue was obtained by transurethral resection of the prostate (TURP) as a result of relieving bladder outflow obstruction.

Immunohistochemistry

Immunohistochemistry for pAR^{ser81} and pAR^{ser213} was performed as described (6, 9, 11, 12). pAR^{ser81} (#07-1375; Merk Millipore, USA) antibody was incubated overnight at 4°C, at 1:4000 and pAR^{ser213} (#IMG-561; Imgenex, USA) was incubated for 1 hour at room temperature at 1:100. A negative control was included with the absence of the primary antibody. Slides were scanned and visualised using Hamamatsu NanoZoomer (Welwyn Garden City, UK) and Slidepath Digital Image Hub, version 4.0.1 (Leica Biosystems, UK). Tissue staining intensity was scored by two independent observers using the weighted histoscore method to assess staining intensity and the percentage of cells with weak, moderate, and strong intensity (13). In brief, the score was calculated by sum of (1 X % cells staining weakly positive) + (2 X % cells staining moderately positive) + (3 X % cells staining strongly positive) with a maximum of 300 (100% strongly stained) and a minimum of 0 (100% with no staining).

Immunofluorescence on Patient Tissue

Immunofluorescence was performed as follows: sections were dewaxed in histoclear and rehydrated through graded alcohol. Antigen retrieval was performed in pH9 Tris-EDTA buffer (5mM Trizma Base, 1mM EDTA) under pressure for 5 minutes. pAR^{ser81} (#07-1375; Merk Millipore, USA) and pAR^{ser213} (#IMG-561; Imgenex, USA) antibodies were incubated together overnight at 4°C, diluted at 1:100 and 1:600 respectively. Staining was captured using the Zeiss LSM 780 Confocal, visualised using Carl Zeiss ZEN 2 blue edition software (Zeiss, Germany), and categorised based on absence and/ or presence of phosphorylated AR antibodies.

Statistical Analysis

Statistical analysis was performed using SPSS version 22. Interclass correlation coefficients (ICCCs) confirmed weighted histoscores were consistent between 2 independent observers. Receiver operator characteristic (ROC) curves identify threshold for low/high expression. Combined expression of pAR^{ser81} and pAR^{ser213} was coded as; low pAR^{ser81} and pAR^{ser213} the both low group, either high pAR^{ser81} or pAR^{ser213} the one high group, and both high pAR^{ser81} and pAR^{ser213} the both high group. Time to biochemical relapse (BR), cancer-specific survival from diagnosis (CSSD) and relapse (CSSR) was analysed using Kaplan Meier log-rank analysis followed by Cox regression, Chi-squared analysis, and Wilcoxon signed-rank test.

TempO-Seq Gene Differential Expression

TempO-Seq gene expression profiling was performed according to manufacturer's directions (17 matched tumour pairs and an additional 6 CRPC tumours) and the Surrogate+Tox panel was used comprising of 2723 genes (BioSpyder Technologies Inc., USA) (14, 15). Data was analysed using the DESeq2 package to compare differentially expressed genes between HN and CR tumours pairs and AR phosphorylation status. Fold change (FC) and p-values were calculated statistically and adjusted for multiple comparisons with $p\text{-value}<0.05$ considered statistically significant. When comparing AR phosphorylation status, due to lack of number an unadjusted $p\text{-value}<0.001$ was considered statistically significant.

Results

Patient characteristics

Clinico-pathological data was collected from 109 patients with matched hormone-naïve (HN) and castrate-resistant (CR) tumour pairs and included age at diagnosis (mean 69, Interquartile Range (IQR) 66-74), Gleason grade at diagnosis (mean 7, IQR 6-9), Gleason grade at relapse (mean 8.55, IQR 8-9), serum PSA concentration at diagnosis (mean 146.51 ng/ml, IQR 8.55-126.18), and serum PSA concentration at relapse (mean 62.95 ng/ml, IQR 4.57-39.50). All patients had biochemical relapse with a mean time to relapse from diagnosis of 3.24 years (IQR 1.58-4.50). Mean cancer specific survival from relapse (CSSR) was 2.7 years (IQR 1.1-3.5 years) and mean cancer specific survival (CSS) was 5.7 years (IQR 3.4-7.2 years) (Supplementary Table 1).

AR phosphorylation expression following the transition from hormone-naïve to castrate-resistant disease

HN nuclear pAR^{ser81} expression ranged from 0-250 weighted histoscore units (WHU) with a median of 100 WHU (interquartile range (IQR) 50-135). ROC curve analysis determined a threshold of 115 WHU that separated pAR^{ser81} expression into high and low. HN pAR^{ser81} expression at diagnosis was not associated with time to biochemical relapse, CSS (p=0.630 and p=0.933 respectively) or clinico-pathological features. Following the development of CR disease, pAR^{ser81} expression decreased (p=0.002) (Figure 1A and B). CR nuclear pAR^{ser81} expression ranged from 0-200 WHU with a median of 90 WHU ((IQR 50-120). ROC curve analysis determined a threshold of 95 WHU that separated pAR^{ser81} expression into high and low. Despite this, 46.7% of CR samples expressed high pAR^{ser81} expression. However, CR pAR^{ser81} expression was not associated with CSSR (p=0.068) (Figure 1C). Furthermore, HN nuclear pAR^{ser213} expression ranged from 0-175 WHU with a median of 11 WHU (IQR 0-80). ROC curve analysis determined a threshold of 9 WHU that separated pAR^{ser213} expression into high and low. HN pAR^{ser213} expression was not associated with time to biochemical relapse, CSS (p=0.150 and p=0.861 respectively) or clinico-pathological features. CR nuclear pAR^{ser213} expression

ranged from 0-200 WHU with a median of 90 WHU ((IQR 40-160). ROC curve analysis determined a threshold of 93 WHU that separated pAR^{ser213} expression into high and low. CR pAR^{ser213} expression increased in 66.3% of patients (p=0.002), with high expression associating with reduced CSSR (p=0.001, HR=2.457 (1.388-4.349)) (Figure 1D, E, and F). High CR pAR^{ser213} expression stratified mean CSSR from 4.44 years in low expressing tumours to 2.54 years in high expressing tumours and was independent in cox regression multivariate analysis when compared with clinico-pathological features (p=0.029, HR=2.618). 5-year survival was reduced from 35% for patients with low pAR^{ser213} expression to 16% for patients with high expression.

Combined castrate-resistant pAR^{ser81} and pAR^{ser213} expression score

High CR pAR^{ser81} and high pAR^{ser213} expression reduced CSSR from 5.73 years to 2.03 years (p=000297) (Figure 2A). Furthermore, 5-year survival was reduced from 47% for patients expressing low of both sites to 7% for patients expressing high of both sites. Following immunofluorescence, 21.7% of CR tumours expressed both pAR^{ser81} and pAR^{ser213} within the same cell. CSSR was reduced from 5.26 years to 1.69 years with 5-year survival reducing from 40% to 22% (p=0.000011) (Figure 2B and C).

Stimulating and inhibiting AR phosphorylation *in vitro*

In LNCaP-AI cells, androgen-dependent stimulation by 10nM DHT induced pAR^{ser81} expression by 30 minutes and 8 hours (p<0.001) (Figure 3A C, E and F), however only a slight increase in pAR^{ser213} was observed (Figure 3B, D, E and F). Androgen-independent stimulation by 10nM EGF induced pAR^{ser81} expression by 5 minutes and 2 hours (Figure 4A, C, E and F) and pAR^{ser213} expression by 30 minutes and 4 hours (p<0.001 and p<0.001 respectively) (Figure 4B, D, E and F). Subsequently, we determined the effects on AR phosphorylation by blocking androgen-dependent by the non-steroidal second-generation AR antagonist Enzalutamide or PI3K-driven phosphorylation by the pan-class PI3K inhibitor BKM120. 10nM Enzalutamide significantly reduced 10nM DHT induced pAR^{ser81} expression and interestingly reduced pAR^{ser213} expression to unstimulated levels (Figure 5A, B and C). Additionally, 10nM BKM120 significantly reduced 10nM EGF induced pAR^{ser81} and pAR^{ser213}

expression (Figure 5D, E and F). Unfortunately, when used as monotherapies, neither 10nM Enzalutamide nor 10nM BKM120 was able to reduce cell viability by 10 days (Figure 5G and H). However, LNCaP-AI cell viability was significantly reduced after 10 days following combining 10nM Enzalutamide and 10nM BKM120 when compared to cells cultured in full media ($p<0.05$) (Figure 5i).

Differentially expressed genes between high and low castrate-resistant AR phosphorylation status

Differential gene expression analysis on 2723 genes, pre-selected for their biological relevance in cancer, was performed on 10 patients with matched HN and CR tumour samples. In CR tumours, 8 genes were differentially expressed (DE) when compared to their matched HN tumour including *KIF11, HIST1H3B, UGT1A10, TYMS,* and *CDKN3* (adjusted p-value<0.005) (Supplementary table 2). Furthermore, expression analysis was performed between high and low AR phosphorylation status at CR. However, sample numbers in each group were low with no genes DE following correction for multiple testing (CR pAR^{ser81}: high n=5 and low=12, CR pAR^{ser213}: high n=7 and low n=13). Therefore, we reduced the threshold for unadjusted p-values for significance to $p<0.001$. At CR, tumours with high pAR^{ser213} expression had 25 genes DE including 18 downregulated and 7 upregulated when compare to low pAR^{ser213} expressing CR tumours ($p<0.001$). DE genes with the lowest p-values were *GSTP1, CAMK2B, ATF5, UQCRFS1,* and *C1R*. The top 3 upregulated genes with the largest absolute log2foldchange are implicated in CaP including *CAMK2B* ($p=6.44x10^{-5}$, log2FC=2.367, lfcSE=0.605) involved in aldosterone synthesis, *HPN* (TMPRSS1) (p=0.00035, log2FC=1.938, lfcSE=0.542) which promotes CaP metastasis, and *AMACR* (p=0.00045, log2FC=2.213, lfcSE=0.631) which is expressed in CaP (Supplementary table 3). However, *MAOA* (p=0.00117, log2FC=-2.073, lfcSE=0.639), involved in epithelial to mesenchymal transition, was the only one gene DE in high versus low CR pAR^{ser81} expression suggesting elevated CR pAR^{ser213} expression might have a stronger effect on AR transcription than CR pAR^{ser81}.

Discussion

Despite the development of new hormonal therapies to treat advanced CaP, such as Abiraterone (Johnson & Johnson) and MDV3100 (Medivation), in the majority of advanced CaPs only temporary disease control is achieved with androgen-independent reactivation of AR commencing 2-3 years after ADT. Therefore, this traditional etiology of androgen-driven disease needs to be revised and the elucidation of molecular mechanisms involved in CRPC is required. It has been hypothesised that various pathways lead to CaP recurrence in hormone-deprived environments. However, with the lack of predictive markers to identify activated pathways, inappropriate treatments are administered, clinical trials fail, and patient survival is not improving despite increases in new therapeutic options.

PI3K activation due to the loss of the tumor suppressor gene, PTEN, highlights a genetic abnormality that induces androgen-independent AR expression in 40-70% of patients (16, 17) . Akt, a downstream member of PI3K, plays vital roles in cancer growth and migration and increases AR transcriptional activity *in vitro* identifying pAR^{ser213} in response to Akt binding (18). Interestingly, it has previously been identified that high pAR^{ser213} expression in this cohort is associated with elevated $pAKT^{ser473}$ at castrate-resistance (6). An additional link between Akt activity and survival during ADT has been identified, therefore promoting CRPC development (19). Furthermore, AR nuclear exportation is influenced by pAR^{ser650} by MAPK signalling, therefore highlighting contributions that signal-transduction cascades play in CaP (4). However, *in vitro* studies using Akt specific and PI3K specific inhibitors show differing results with both reduced and increased AR expression being reported (20). Therefore, this study compared a marker of traditional androgen-dependent activation (pAR^{ser81}) with a controversial marker of androgen-independent activation (pAR^{ser213}) and determined their utility as individual and combined biomarkers.

In this cohort, following the development of CR disease, 8 genes were DE when compared to their matched HN tumour with the majority involved in the cell cycle including *CDK1* (M-phase),

CDKN3 (cell-cycle regulator), *TYMS* (S-phase), and *HMMR* (mitotic spindle integrity) (21-24). Interestingly, upregulated *CDK1* in CR tumours is linked to enhancing CR AR and pAR^{ser81} expression in response to low androgen levels (25). Subsequently, in Figure 1 we observed 46.7% of CR tumours with an elevation in pAR^{ser81} expression and a reduced in CSSR. In LNCaP-AI cells, we induced pAR^{ser81} expression by 10nM DHT and subsequently inhibited expression following 10nM Enzalutamide treatment. However, no effect of cell viability was observed.

High CR pAR^{ser213} expression associated with reduced CSSR by 1.9 years (p=0.001) and suggests that following ADT the AR is reactivated androgen-independently. However, contradictory to our findings of decreased survival, it has been reported that pAR^{ser213} in response to Akt can lead to ligand dissociation and degradation of AR (26). Furthermore, pAR^{ser213} in response to Mdm2 results in ubiquitination and degradation of AR and its splice variant AR-V7 (27). Following transcriptomic analysis, multiple genes were dysregulated in high CR pAR^{ser213} expressing tumours. However, due to lack of numbers unadjusted p-values were assessed due to their biological relevance. *HPN,* which codes for hepsin, is overexpressed in up to 90% of CaPs often >10-fold (28, 29). We observed almost a 2-fold increase in *HPN* in high CR pAR^{ser213} expressing tumours and not in high pAR^{ser81} expressing tumours. Furthermore, *HPN* correlates with high Gleason grade and poor clinical outcome (30, 31). Additionally, *GSTP1* was underrepresented in high pAR^{ser213} expressing tumours, a gene involved in reducing oxidative damage. However, when silenced *GSTP1* can promote CaP initiation in 90-95% of CaPs suggesting pAR^{ser213} represents an aggressive phenotype.

ErbB family receptors are involved in CaP tumourigenesis and progression, with aberrant associations observed during the development of CR disease and loss of androgen signaling (3). HER2 overexpression has been reported in CaP progression much like breast cancer, another hormone sensitive/refractory disease (32). HER2 inhibitors have shown to reduce recurrence by up to 50% in HER2 positive breast cancers, with the hope of HER specific inhibitors similarly reducing CaP progression (33, 34). However, overexpression of EGFR is not associated with CaP initiation, differentiation, or positive margins but with progression and castrate-resistance (35-37).

Interestingly, as a result of EGFRvIII expression and subsequent activation of PI3K/Akt, increased proliferation and cell cycle progression has been observed. This signalling reduces the levels of the cyclin-dependent kinase inhibitor, $p27^{KIP1}$, a known inhibitor of the transition from G1 to S phase within the cell cycle in glioblastoma (38). Interestingly, EGFRvIII associates with reduced expression of CDK inhibitors and is hypothesised to result in elevated CDK expression and ultimately overexpression of pAR^{ser81}. Following 10nM EGF stimulation, we observed a significant induction of pAR^{ser81} an pAR^{ser213} expression, further adding to weight to a potential mechanism in which pAR^{ser81} expression reactivates AR in CR CaP. Additionally, when LNCaP-AI cells were treated with 10nM BKM120, a significant reduction in EGF induced pAR^{ser81} and pAR^{ser213} expression was observed.

Due to the promiscuity of AR activation, we have hypothesized that AR activation at multiple sites would have a cumulative prognostic effect. When patients expressed both pAR^{ser81} and pAR^{ser213} at relapse they had a reduced CSSR of 3.71 years (p=0.000297). This significantly increased the prognostic power of these markers when compared alone to patient survival (pAR^{ser81} p=0.068, and pAR^{ser213} p=0.001). Furthermore, patients expressing pAR^{ser81} and pAR^{ser213} within the same cell via immunofluorescence resulted in a reduced CSSR of 3.57 years (p=0.00011).

Due to a feedback loop observed between AR and PI3K/AKT cascade, the use of anti-androgens and PI3K inhibitors as monotherapies have lacked efficacy with no significant reduction in cell viability observed in LNCaP-AI cells following 10nM Enzalutamide or 10nM BKM120 (Figure 5G and H). However, when targeting both androgen-depenedent and PI3K-driven AR activation using 10nM enzalutamide and 10nM BKM120, cell viability signifincatly reduced in LNCaO-AI cells. Therefore, we have hypothesise that patients expressing pAR^{ser81} and pAR^{ser213} expression within the same cell would benefit from this dual therpauetic approach and improve the efficacy of the clinical trial by Armstrong *et al* (8). However, LNCaP AI cells harbour multiple mutations including T878A, F876L, and F877L within the ligand binding domain portion of the AR, resulting in a broader ligand-binding domain pocket which could lead to AR activation by other stimuli such as estrogen and potential agonistic effects following anti-androgen treatment (39-41). Therefore, the effects seen in

LNCaP AI cells in response to stimulation and/ inhibition may only represent a subgroup of prostate cancers with such mutations and needs to be performed in further models to validate results.

To conclude, further elucidation of these biomarkers are required to determine their localisation/co-localisation and whether combining pAR^{ser81} and pAR^{ser213} will provide any further understanding and/ or prognostic power. In addition, the use of various drug combinations with anti-androgens such as Enzaultamide and PI3K/Akt inhibitors such BKM120 on patients depending on their AR phosphorylation status will be further explored to determine correct timing and treatment stratergies for patients that may benefit from early intervention.

Acknowldgments

We thank Prostate Cancer UK for funding the research presented. We would like to acknowledge the Glasgow Research Tissue Facility and Glasgow Biorepository for supporting this study.

Conflicts of interest

The authors declare no potential conflicts of interest

References

1. Siegel RL, Miller KD, Jemal A. Cancer statistics, 2016. CA Cancer J Clin. 2016;66(1):7-30.
2. Tilki D, Schaeffer EM, Evans CP. Understanding Mechanisms of Resistance in Metastatic Castration-resistant Prostate Cancer: The Role of the Androgen Receptor. Eur Urol Focus. 2016;2(5):499-505.
3. Ponguta LA, Gregory CW, French FS, Wilson EM. Site-specific androgen receptor serine phosphorylation linked to epidermal growth factor-dependent growth of castration-recurrent prostate cancer. J Biol Chem. 2008;283(30):20989-1001.
4. Hsu FN, Chen MC, Chiang MC, Lin E, Lee YT, Huang PH, et al. Regulation of androgen receptor and prostate cancer growth by cyclin-dependent kinase 5. J Biol Chem. 2011;286(38):33141-9.
5. Górowska-Wójtowicz E, Hejmej A, Kamińska A, Pardyak L, Kotula-Balak M, Dulińska-Litewka J, et al. Anti-androgen 2-hydroxyflutamide modulates cadherin, catenin and androgen receptor phosphorylation in androgen-sensitive LNCaP and androgen-independent PC3 prostate cancer cell lines acting via PI3K/Akt and MAPK/ERK1/2 pathways. Toxicol In Vitro. 2017;40:324-35.
6. McCall P, Gemmell LK, Mukherjee R, Bartlett JM, Edwards J. Phosphorylation of the androgen receptor is associated with reduced survival in hormone-refractory prostate cancer patients. Br J Cancer. 2008;98(6):1094-101.
7. Heimberger AB, Hlatky R, Suki D, Yang D, Weinberg J, Gilbert M, et al. Prognostic effect of epidermal growth factor receptor and EGFRvIII in glioblastoma multiforme patients. Clin Cancer Res. 2005;11(4):1462-6.
8. Armstrong AJ, Halabi S, Healy P, Alumkal JJ, Winters C, Kephart J, et al. Phase II trial of the PI3 kinase inhibitor buparlisib (BKM-120) with or without enzalutamide in men with metastatic castration resistant prostate cancer. Eur J Cancer. 2017;81:228-36.
9. Willder JM, Heng SJ, McCall P, Adams CE, Tannahill C, Fyffe G, et al. Androgen receptor phosphorylation at serine 515 by Cdk1 predicts biochemical relapse in prostate cancer patients. Br J Cancer. 2013;108(1):139-48.
10. Patek S, Willder J, Heng J, Taylor B, Horgan P, Leung H, et al. Androgen receptor phosphorylation status at serine 578 predicts poor outcome in prostate cancer patients. Oncotarget. 2017;8(3):4875-87.
11. Bartlett JM, Brawley D, Grigor K, Munro AF, Dunne B, Edwards J. Type I receptor tyrosine kinases are associated with hormone escape in prostate cancer. J Pathol. 2005;205(4):522-9.
12. Edwards J, Traynor P, Munro AF, Pirret CF, Dunne B, Bartlett JM. The role of HER1-HER4 and EGFRvIII in hormone-refractory prostate cancer. Clin Cancer Res. 2006;12(1):123-30.
13. Kirkegaard T, Edwards J, Tovey S, McGlynn LM, Krishna SN, Mukherjee R, et al. Observer variation in immunohistochemical analysis of protein expression, time for a change? Histopathology. 2006;48(7):787-94.
14. Trejo CL, Profile VO, Babić M, Imler E, Gonzalez M, Bibikov S, et al. Extraction-Free Whole Transcriptome Gene Expression Analysis of FFPE Sections and Histology-Directed Subareas of Tissue. bioRxiv. 2018.
15. Mav D, Shah RR, Howard BE, Auerbach SS, Bushel PR, Collins JB, et al. A hybrid gene selection approach to create the S1500+ targeted gene sets for use in high-throughput transcriptomics. PLoS One. 2018;13(2):e0191105.
16. Thorpe LM, Yuzugullu H, Zhao JJ. PI3K in cancer: divergent roles of isoforms, modes of activation and therapeutic targeting. Nat Rev Cancer. 2015;15(1):7-24.
17. Majumder PK, Sellers WR. Akt-regulated pathways in prostate cancer. Oncogene. 2005;24(50):7465-74.
18. Lin HK, Wang L, Hu YC, Altuwaijri S, Chang C. Phosphorylation-dependent ubiquitylation and degradation of androgen receptor by Akt require Mdm2 E3 ligase. EMBO J. 2002;21(15):4037-48.

19. Wen Y, Hu MC, Makino K, Spohn B, Bartholomeusz G, Yan DH, et al. HER-2/neu promotes androgen-independent survival and growth of prostate cancer cells through the Akt pathway. Cancer Res. 2000;60(24):6841-5.
20. Blom S, Mäki-Teeri P, Erickson A, Paavolainen L, Mirtti T, Rannikko A, et al. Abstract: PI3K/Akt activity regulates androgen receptor expression and predicts poor clinical outcome in non-metastatic hormone-naïve prostate cancer. Cancer Research. 2017;77:5732-3.
21. Wang Q, Li W, Zhang Y, Yuan X, Xu K, Yu J, et al. Androgen receptor regulates a distinct transcription program in androgen-independent prostate cancer. Cell. 2009;138(2):245-56.
22. Yu C, Cao H, He X, Sun P, Feng Y, Chen L, et al. Cyclin-dependent kinase inhibitor 3 (CDKN3) plays a critical role in prostate cancer via regulating cell cycle and DNA replication signaling. Biomed Pharmacother. 2017;96:1109-18.
23. Zhao H, Whitfield ML, Xu T, Botstein D, Brooks JD. Diverse effects of methylseleninic acid on the transcriptional program of human prostate cancer cells. Mol Biol Cell. 2004;15(2):506-19.
24. Maxwell CA, McCarthy J, Turley E. Cell-surface and mitotic-spindle RHAMM: moonlighting or dual oncogenic functions? J Cell Sci. 2008;121(Pt 7):925-32.
25. Chen S, Xu Y, Yuan X, Bubley GJ, Balk SP. Androgen receptor phosphorylation and stabilization in prostate cancer by cyclin-dependent kinase 1. Proc Natl Acad Sci U S A. 2006;103(43):15969-74.
26. McClurg UL, Summerscales EE, Harle VJ, Gaughan L, Robson CN. Deubiquitinating enzyme Usp12 regulates the interaction between the androgen receptor and the Akt pathway. Oncotarget. 2014;5(16):7081-92.
27. Li Y, Xie N, Gleave ME, Rennie PS, Dong X. AR-v7 protein expression is regulated by protein kinase and phosphatase. Oncotarget. 2015;6(32):33743-54.
28. Dhanasekaran SM, Barrette TR, Ghosh D, Shah R, Varambally S, Kurachi K, et al. Delineation of prognostic biomarkers in prostate cancer. Nature. 2001;412(6849):822-6.
29. Stamey TA, Warrington JA, Caldwell MC, Chen Z, Fan Z, Mahadevappa M, et al. Molecular genetic profiling of Gleason grade 4/5 prostate cancers compared to benign prostatic hyperplasia. J Urol. 2001;166(6):2171-7.
30. Magee JA, Araki T, Patil S, Ehrig T, True L, Humphrey PA, et al. Expression profiling reveals hepsin overexpression in prostate cancer. Cancer Res. 2001;61(15):5692-6.
31. Chen Z, Fan Z, McNeal JE, Nolley R, Caldwell MC, Mahadevappa M, et al. Hepsin and maspin are inversely expressed in laser capture microdissectioned prostate cancer. J Urol. 2003;169(4):1316-9.
32. Craft N, Shostak Y, Carey M, Sawyers CL. A mechanism for hormone-independent prostate cancer through modulation of androgen receptor signaling by the HER-2/neu tyrosine kinase. Nat Med. 1999;5(3):280-5.
33. Schroeder RL, Stevens CL, Sridhar J. Small molecule tyrosine kinase inhibitors of ErbB2/HER2/Neu in the treatment of aggressive breast cancer. Molecules. 2014;19(9):15196-212.
34. Day KC, Lorenzatti Hiles G, Kozminsky M, Dawsey SJ, Paul A, Broses LJ, et al. HER2 and EGFR Overexpression Support Metastatic Progression of Prostate Cancer to Bone. Cancer Res. 2017;77(1):74-85.
35. Shah RB, Ghosh D, Elder JT. Epidermal growth factor receptor (ErbB1) expression in prostate cancer progression: correlation with androgen independence. Prostate. 2006;66(13):1437-44.
36. Traish AM, Morgentaler A. Epidermal growth factor receptor expression escapes androgen regulation in prostate cancer: a potential molecular switch for tumour growth. Br J Cancer. 2009;101(12):1949-56.
37. DeHaan AM, Wolters NM, Keller ET, Ignatoski KM. EGFR ligand switch in late stage prostate cancer contributes to changes in cell signaling and bone remodeling. Prostate. 2009;69(5):528-37.
38. Narita Y, Nagane M, Mishima K, Huang HJ, Furnari FB, Cavenee WK. Mutant epidermal growth factor receptor signaling down-regulates p27 through activation of the phosphatidylinositol 3-kinase/Akt pathway in glioblastomas. Cancer Res. 2002;62(22):6764-9.

428 39. Gottlieb B, Beitel LK, Nadarajah A, Paliouras M, Trifiro M. The androgen receptor gene
429 mutations database: 2012 update. Hum Mutat. 2012;33(5):887-94.
430 40. Hara T, Miyazaki J, Araki H, Yamaoka M, Kanzaki N, Kusaka M, et al. Novel mutations of
431 androgen receptor: a possible mechanism of bicalutamide withdrawal syndrome. Cancer Res.
432 2003;63(1):149-53.
433 41. Korpal M, Korn JM, Gao X, Rakiec DP, Ruddy DA, Doshi S, et al. An F876L mutation in
434 androgen receptor confers genetic and phenotypic resistance to MDV3100 (enzalutamide). Cancer
435 Discov. 2013;3(9):1030-43.

436

437

Tables and Figures

Figure 1: Androgen receptor phosphorylation status between hormone-naïve and castrate-resistant prostate cancer. (A) High and low pAR^{ser81} expression in prostate cancer (B) pAR^{ser81} expression significantly reduces following the development of castrate-resistant disease (C) High pAR^{ser81} expression does not significantly reduce cancer specific survival from relapse (D) High and low pAR^{ser213} expression in prostate cancer (E) pAR^{ser213} expression significantly increases following the development of castrate-resistant disease (F) High pAR^{ser213} expression significantly reduced cancer specific survival from relapse. Wilcoxon signed-rank tests and Kaplan Meier survival curves with log-rank tests were considered significant if P<0.05. Censor lines were included to indicate loss of patient follow up.

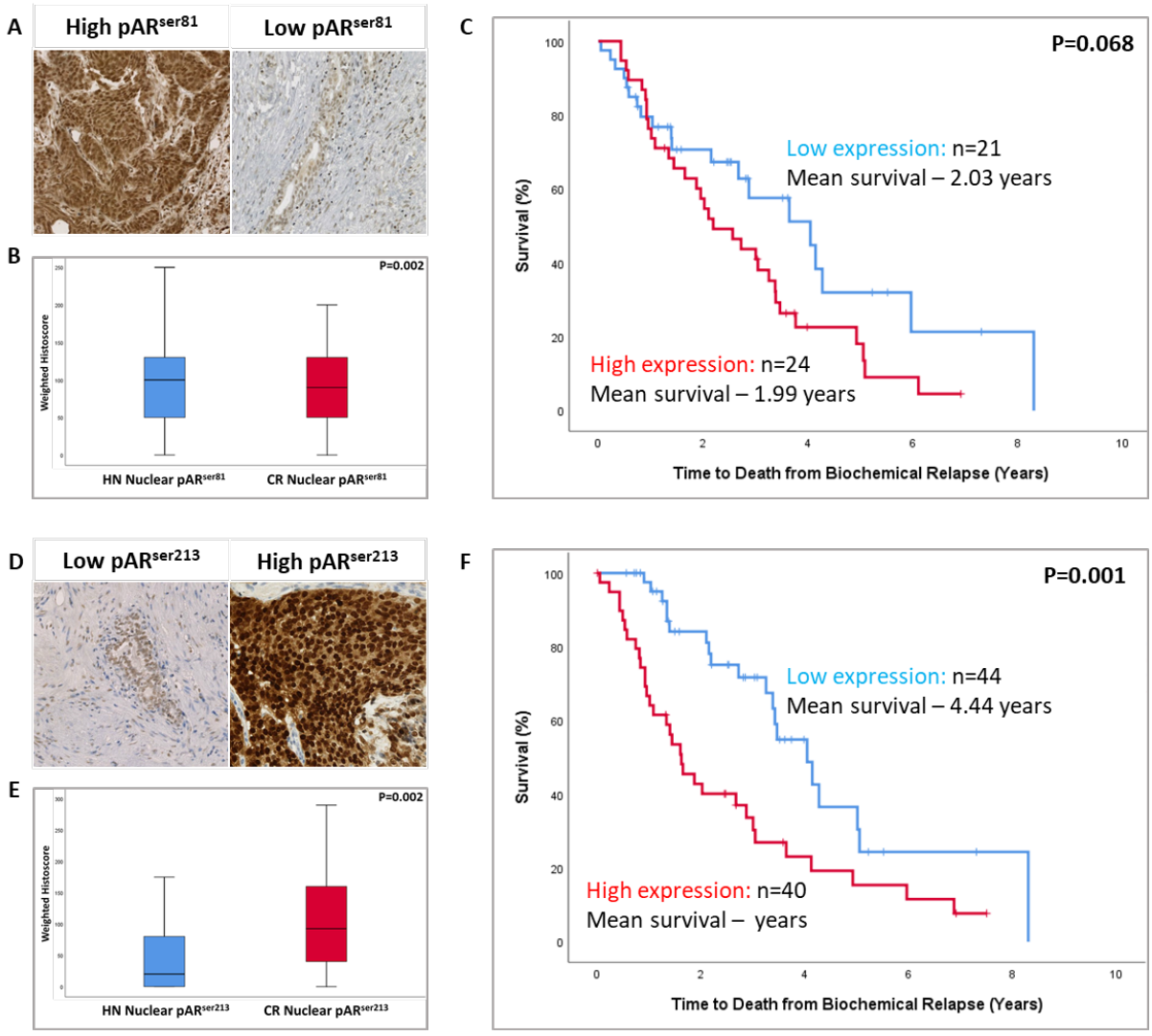

Figure 2: Combined pAR^{ser81} and pAR^{ser213} expression in castrate-resistant tumours. (A) Following immunohistochemistry, castrate-resistant patients with high pAR^{ser81} and high pAR^{ser213} expression had significantly reduced cancer specific survival from relapse (B) Following dual immunofluorescence, castrate-resistant patients expressing pAR^{ser81} and pAR^{ser213} within the same cell had a significantly reduced cancer specific survival from relapse (C) Example of castrate-resistant tumours expressing only pAR^{ser81}, only pAR^{ser213}, and combined pAR^{ser81} an pAR^{ser213} within the same cell. Kaplan Meier survival curves with log-rank tests were considered significant if P<0.05. Censor lines were included to indicate loss of patient follow up. Blue fluorescence DAPI was used as a nuclear counterstain. Scale bar represents 20µm.

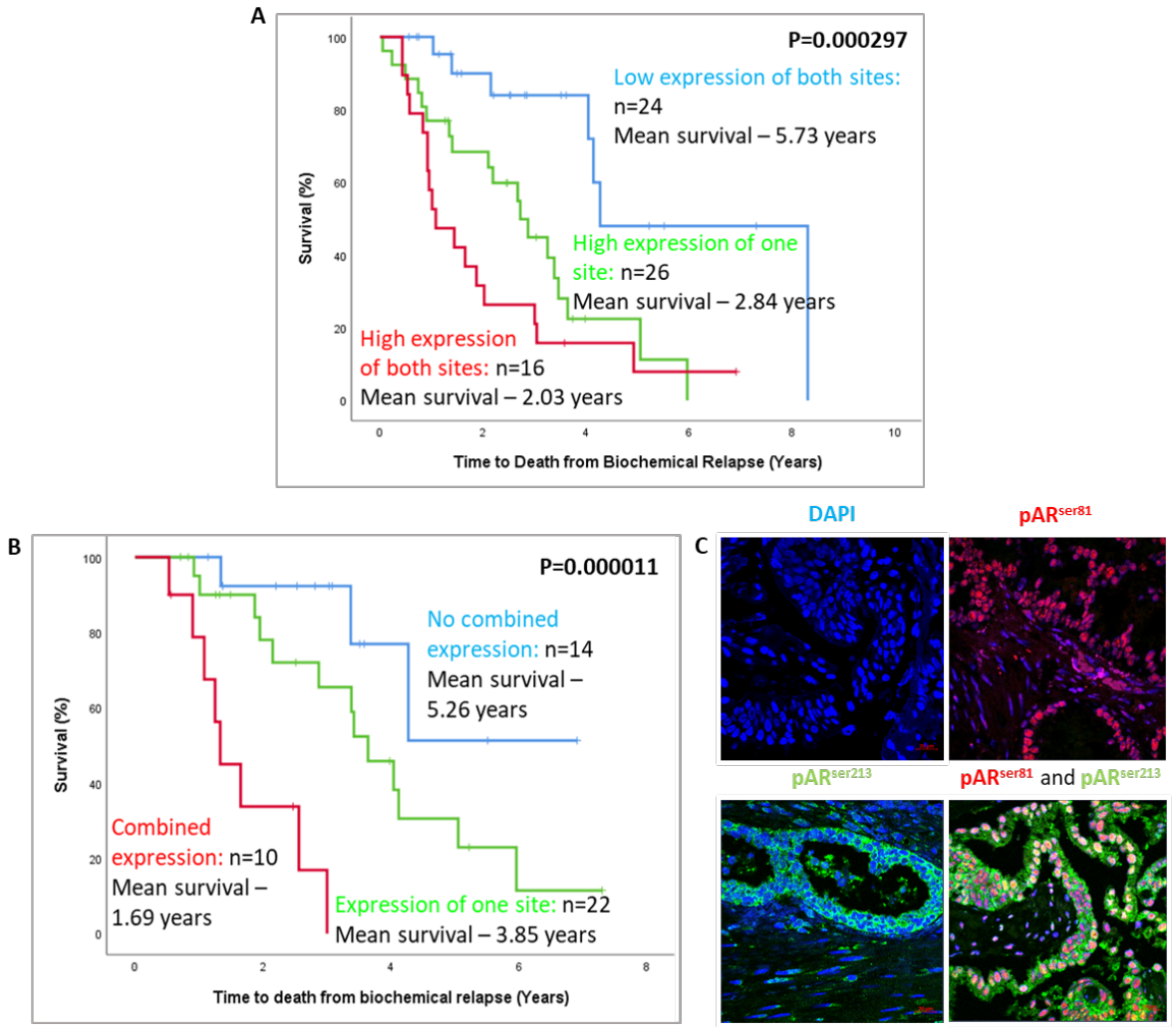

Figure 3: Stimulating androgen-dependent androgen receptor signalling in LNCaP-AI cells. (A and B) Exposure to 10 nM DHT over 1 hour significantly increased pAR^{ser81} expression by 30 minutes but not pAR^{ser213} expression (C and D) Exposure to 10 nM DHT over 12 hours significantly increased pAR^{ser81} expression by 8 hours but not pAR^{ser213} expression (E and F) Quantification of AR phosphorylation pixel intensity following 1 and 12 hour 10 nM DHT stimulation. Each experiment was repeated to N=3. DAPI was included as a nuclear stain and scale bars represent 50 µm. Fluorescence expression was quantified and compared to a control containing no primary antibody. Error bars represent standard error and statistical analysis was performed using a one-way ANOVA with Bonferroni correction and Dunnett's test. ** indicate a significant difference of P<0.001.

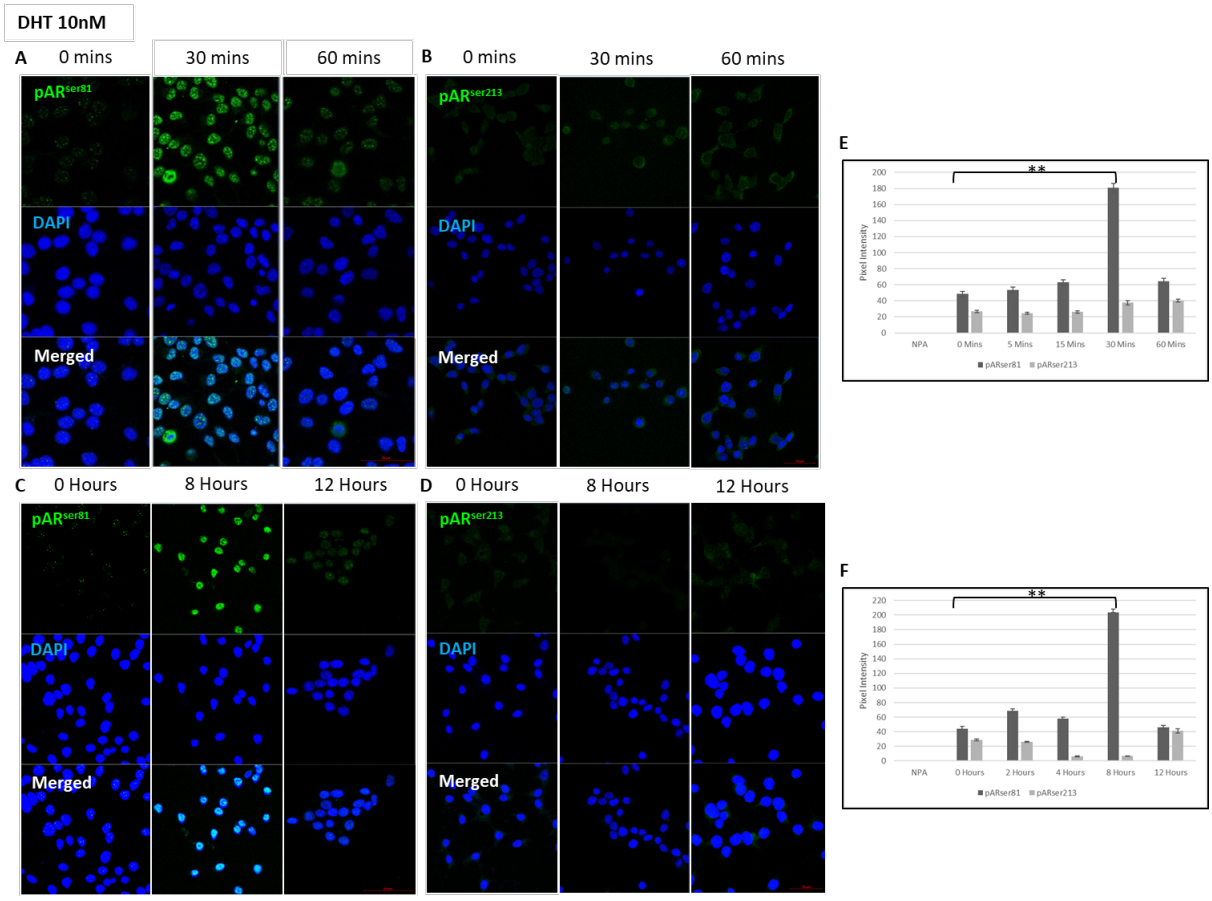

Figure 4: Stimulating androgen-independent androgen receptor signalling in LNCaP-AI cells. (A and B) Exposure to 10 nM EGF over 1 hour significantly increased pAR^{ser81} expression by 5 minutes and pAR^{ser213} expression by 30 minutes (C and D) Exposure to 10 nM EGF over 12 hours significantly increased pAR^{ser81} expression by 2 hours and pAR^{ser213} expression by 4 hours (E and F) Quantification of AR phosphorylation pixel intensity following 1 and 12 hour 10 nM EGF stimulation. Each experiment was repeated to N=3. DAPI was included as a nuclear stain and scale bars represent 50 µm. Fluorescence expression was quantified and compared to a control containing no primary antibody. Error bars represent standard error and statistical analysis was performed using a one-way ANOVA with Bonferroni correction and Dunnett's test. ** indicate a significant difference of P<0.001.

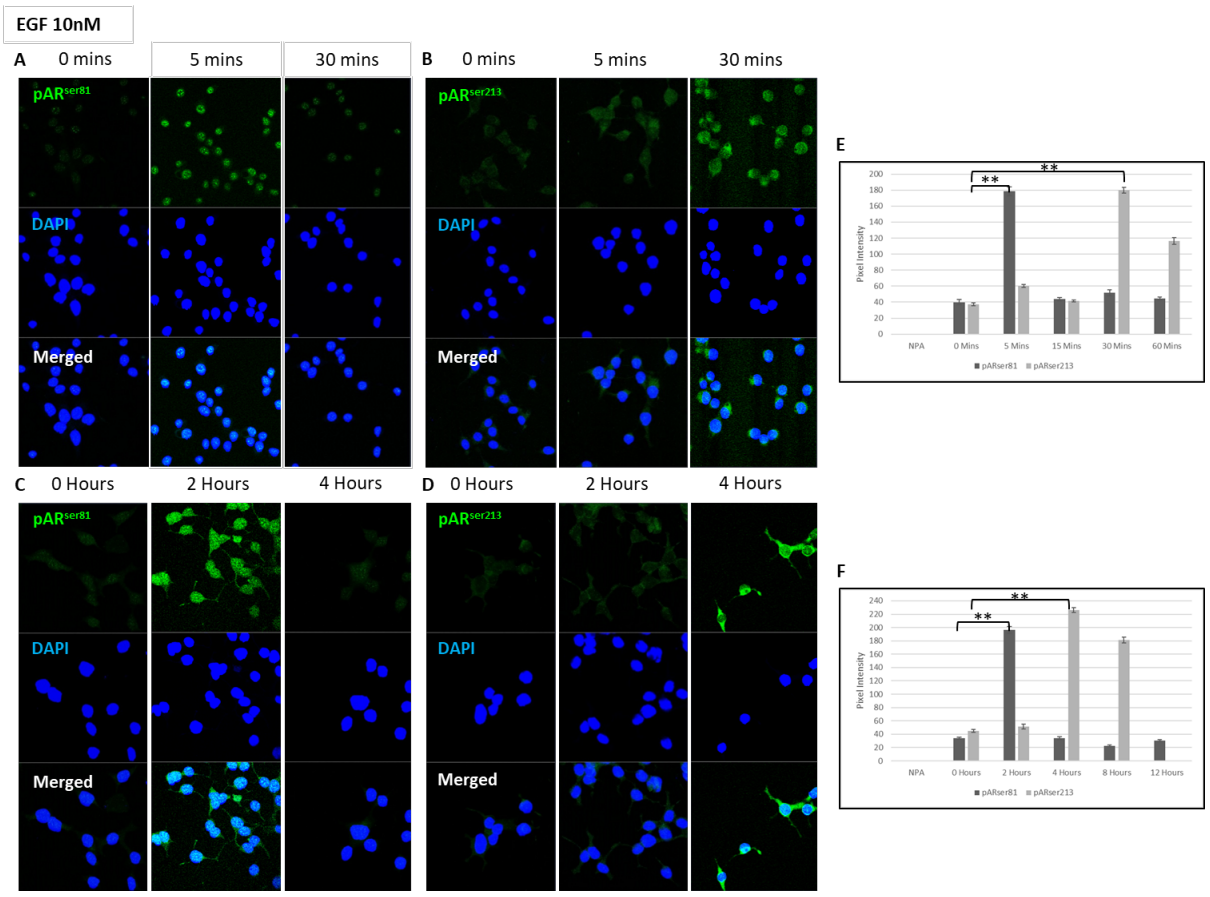

Figure 5: Inhibiting androgen receptor signalling in LNCaP-AI cells. (A,B and C) 10 nM Enzalutamide treatment significantly reduced 10 nM DHT induced pAR^{ser81} expression but not pAR^{ser213} expression (D, E and F) 10 nM BKM120 treatment significantly reduced 10 nM EGF induced pAR^{ser81} and pAR^{ser213} expression (G) No effect on LNCaP-AI cell viability was observed following 10 nM Enzalutamide treatment over 10 days (H) No effect on LNCaP-AI cell viability was observed following 10 nM BKM120 treatment over 10 days (I) Combined treatment with 10 nM Enzalutamide and 10 nM BKM120 significantly reduced LNCaP-AI cell viability by 10 days. Each experiment was repeated to N=3. DAPI was included as a nuclear stain and scale bars represent 50 µm. Fluorescence expression was quantified and compared to a control containing no primary antibody. Error bars represent standard error and statistical analysis was performed using a one-way ANOVA with Bonferroni correction and Dunnett's test. * and ** indicate a significant difference of $P<0.05$ and $P<0.001$ respectively.

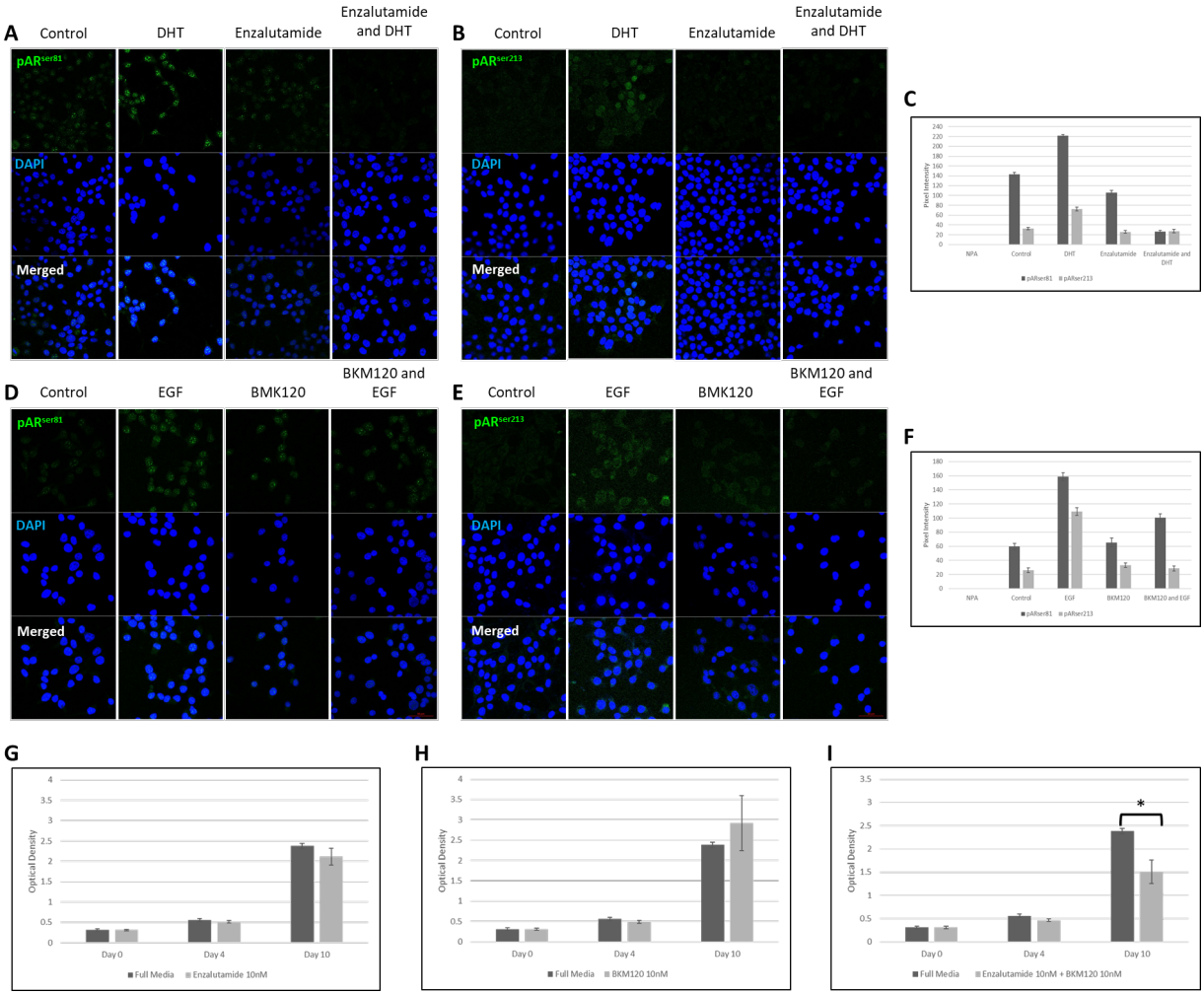

Supplementary table 1: Clinico-pathological cohort characteristics and relationship with clinical outcome measures. The number of patients in each group are described along with the significance to time to biochemical relapse (BR), cancer specific survival from relapse (CSSR), and cancer specific survival (CSS). Kaplan Meier survival curves with log-rank tests were considered significant if P<0.05.

Clinico-pathological characteristics	**Patient Numbers n (%) Total n = 109**	**Clinical Outcome Significance**
Age at Diagnosis (≤70/>70 years/ Missing)	61 (35%)/ 46 (26%)/ 68 (39%)	CSS: P=0.246 BR:P=0.210
Gleason Grade at Diagnosis (<7/ 7/ >7/ Missing)	27 (15%), 24 (14%), 49 (28%), 75 (43%)	**CSS: P=0.001** BR: P=0.031

Serum PSA Concentration at Diagnosis (<10/ 10-20/ >20/ Missing)	26 (15%), 11 (6%), 61 (35%), 77 (44%)	CSS: P=0.380 BR: P=0.058
Metastases at Diagnosis (No/ Yes/ Missing)	68 (39%), 30 (17%), 77 (44%)	**CSS: P=0.000077** **BR: P=0.007**
Gleason Grade at Relapse (<7/ 7/ >7/ Missing)	5 (3%), 12 (7%), 84 (48%), 74 (42%)	CSSR:P=0.675
Serum PSA Concentration at Relapse (<10/ 10-20/ >20/ Missing)	24 (14%), 6 (3%), 28 (16%), 117 (67%)	**CSSR: P=0.023**
Metastases at Relapse (No/ Yes/ Missing)	20 (11%), 56 (32%), 99 (57%)	**CSSR: P=0.000442**

502

Supplementary table 2: Differential gene expression analysis between hormone-naïve and castrate-resistant prostate cancer. 8 gene were significantly upregulated in castrate-resistant tumours when compared to their matched hormone-naive tumour. P>0.05 was considered significant for adjusted p-values.

Gene	**Log2FoldChange**	**lfcSE**	**P-Value**	**Adjusted P-Value**
KIF11_3588	1.606687	0.324044	7.11E-07	0.002094
HIST1H3B_12576	1.717355	0.391572	1.16E-05	0.017011
UGT1A10_28864	2.229366	0.539585	3.60E-05	0.022069
TYMS_21327	1.304365	0.318614	4.24E-05	0.022069
CDKN3_17690	1.660734	0.406628	4.42E-05	0.022069
CDK1_1196	2.053808	0.503347	4.50E-05	0.022069
HMMR_3040	1.194755	0.300411	6.98E-05	0.029344
CENPW_1256	1.040229	0.268995	0.00011	0.04053

Supplementary table 3: Differential gene expression analysis between high and low pAR^{ser213} expression in castrate-resistant tumours. 25 genes were differentially expressed in high pAR^{ser213} expressing castrate-resistant tumours when compared to low pAR^{ser213}. 18 genes were downregulated and 7 genes were upregulated. P>0.001 was considered significant for unadjusted p-values.

Gene	Log2foldchange	LfcSE	P-Value	Adjusted P-Value
GSTP1_24644	-2.3134	0.578919	6.44E-05	0.04741
CAMK2B_26957	2.36701	0.60481	9.09E-05	0.04741
ATF5_501	1.34956	0.346107	9.65E-05	0.04741
UQCRFS1_7566	0.86679	0.23363	0.00021	0.06063
C1R_871	-1.3565	0.369807	0.00024	0.06063
CASP1_26966	-1.384	0.38356	0.00031	0.06063
HPN_25853	1.93783	0.541716	0.00035	0.06063
KRT15_19413	-3.248	0.910927	0.00036	0.06063
ARHGAP8_26848	1.34436	0.37758	0.00037	0.06063
AMACR_14170	2.21333	0.630683	0.00045	0.0662
LOC100510495_28176	-1.3128	0.379924	0.00055	0.06728
MYLK_4414	-1.9181	0.555136	0.00055	0.06728
C3_886	-1.9042	0.554412	0.00059	0.06728
SMAD3_27880	-0.9936	0.292956	0.0007	0.06982
ID1_14943	-1.8632	0.550338	0.00071	0.06982
IGFBP6_26498	-1.8047	0.542909	0.00089	0.07082
CFH_27007	-1.4165	0.426346	0.00089	0.07082

FGF2_2405	-1.661	0.500727	0.00091	0.07082
CCND1_1062	-0.7696	0.232679	0.00094	0.07082
HPN_3091	1.86637	0.565271	0.00096	0.07082
SCARB1_6117	1.08261	0.333161	0.00116	0.08114
FLNA_25912	-1.4413	0.448573	0.00131	0.0817
BMP4_737	-1.2925	0.403309	0.00135	0.0817
ZEB2_23804	-1.1773	0.367524	0.00136	0.0817
TPSB2_17547	-1.5698	0.490942	0.00139	0.0817

513

514